Bandwidth Enhancement Techniques for Large-Area VLC Receivers

***Abstract*—The work reports, for the first time, the use of Linvill's negative impedance converter (NIC) to generate negative resistance and inductance for the purpose of extending the bandwidth of optical receivers used in visible light communication (VLC). The work shows that the bandwidth-limiting series resistance, inherent in large-area photodiodes, can be compensated by using a simple NIC circuitry generating a compensating negative resistance in series with a negative inductive reactance. Mathematical derivations and simulations are verified by experimental results showing a bandwidth extension of up to 400% when used with only minimal additional circuit elements.**

***Index Terms*—Negative impedance converters, negative resistance, photodiodes, visible light communication.**

I. Introduction

A long-standing problem facing VLC systems is improving data transmission speeds, considering the low modulation bandwidth of commercially available optoelectronic devices of the transmitter and the receiver [1]. At the receiver, the challenge is in capturing sufficient light to ensure correct detection of the transmitted information. This is a difficult challenge for two reasons; firstly, the nature of the free space channel, wherein loss is proportional to the square of the transmission distance. Second, most photodiodes operating in the visible range are silicon diodes, which have poor responsivity in the relevant frequency range, limiting the converted photocurrent [2]. Therefore, to boost the received signal power, a combination of a large-area photodiode and a high-gain transimpedance amplifier (TIA) is desirable to detect the transmitted signal correctly. Unfortunately, large-area photodiodes are associated with high junction capacitance C_{pd}, which limits the receiver bandwidth, particularly when followed by high input impedance or traditional 50 Ω TIAs.

To overcome the photodiode bandwidth limitation in VLC, TIAs adopting negative feedback [3], and others with low input impedance configurations, such as the regulated cascode (RGC) [4–7] have been proposed. For instance, work in [6] reports a modified RGC TIA for large-area photodiodes, predicted a bandwidth of 200 MHz at 2 kΩ transimpedance gain with an equivalent C_{pd} of 300 pF. Such remarkable bandwidth performance at an exceptionally high C_{pd} is a virtue of the ultra-low input impedance of the RGC TIA. Nevertheless, such TIA designs are based on a simplified photodiode equivalent circuit, which models the photodiode behaviour simply as a current source in parallel with a shunt capacitance C_{pd}. This overlooks other bandwidth-limiting effects arising from intrinsic elements of the photodiode or extrinsic parasitic factors. Alas, discarding the bandwidth-limiting effects of such elements and assuming a simplified photodiode equivalent circuit model was shown to be insufficient in predicting the photodiode behaviour accurately and, as such, may mislead the design of the TIA [8].

The equivalent circuit model of photodiodes is crucially important in optimising TIA performance. Work in [8–10] reports full and accurate high-frequency modelling and parameter extraction of photodiodes, accounting for all intrinsic photodiode elements such as its series resistance R_s, pad capacitance C_p and extrinsic feed-line inductance L_s. In particular, work in [8], reports modelling and parameter extraction for large-area photodiodes akin to devices used in VLC. The photodiode modelling identifies R_s as a major contributor to the bandwidth limitation of VLC receivers, especially when employing a combination of a large-area photodiode and low input impedance TIA. Such resistance is often in the range of few ohms; therefore, it became a convention for circuit designers to ignore it [3–7, 11], since it is assumed that such resistance has a negligible effect on the TIA performance. Nevertheless, such resistance adds to the TIA input resistance and, in turn, inflicts an additional bandwidth-limiting factor for optical receivers.

In this work, we propose a new method for using negative impedance converters (NICs) to enhance the bandwidth of optical receivers utilising large-area photodiodes. The idea is to neutralise the bandwidth-limiting effect of the photodiode series resistance by introducing an in-series negative resistance between the photodiode and the TIA, reducing the net input resistance at the TIA and, thereby, enhancing the receiver bandwidth. First, we demonstrate a negative resistance circuit based on the well-known Linvill NIC [12]. Subsequently, the application of NICs to extend the bandwidth of photodiodes is demonstrated in conjunction with a low input impedance RGC TIA.

II. Design of the Negative Impedance Converter

A NIC is defined as a two-port network that presents negative impedance at one port when terminated by the corresponding load impedance at the other port [12]. NICs can be devised in various ways, Linvill cross-coupled pair [12–14], other two-transistor configurations [15, 16] and using operational amplifiers [17]. Essentially, they all apply positive feedback to manipulate the voltage-current relation of a load impedance to achieve phase inversion at the output port and, as such, generate negative impedance.

NICs can generate either negative resistance, negative inductance or negative capacitance. Due to their attractive capability of creating unconventional impedances, such networks are widely used to improve the performance of various applications. For example, enhancing the bandwidth of amplifiers by neutralising bandwidth-limiting capacitances [18, 19], broadband matching of small electrical antennas to overcome the gain-bandwidth restriction [20, 21] and more

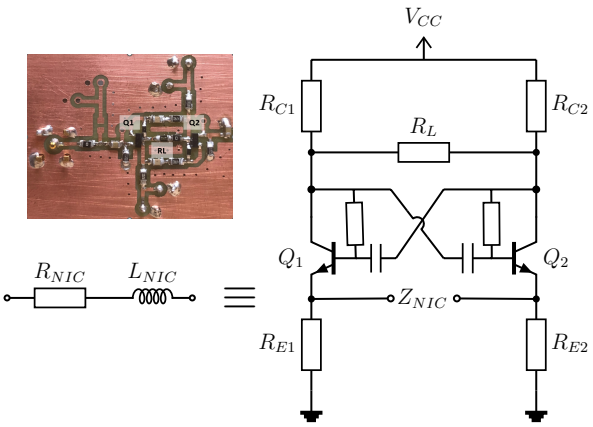

Fig. 1: Linvill OCS NIC generating floating negative resistance, inset: Fabricated PCB

recently, in extending the bandwidth of optical transmitters by neutralising the bandwidth-limiting capacitance of light emitting diodes (LEDs) [16].

In this work, the floating negative resistance element generation is achieved using the Linvill NIC shown in Fig. 1. The circuit is one of two varieties introduced by Linvill in [12], which are classified according to their stability as short circuit stable (SCS) and open circuit stable (OCS) NICs, in balanced and unbalanced forms suggesting the negative impedance generated is either floating or grounded impedance, respectively. A grounded-type NICs are suitable to be connected as a shunt element, whereas the floating-type NICs are to be connected as in-series element to a network.

Fig. 1 shows the OCS balanced Linvill NIC, which is based on a cross coupled pair of transistors Q_1 and Q_2, where the bases of each transistor is connected to the collector of the other to form a positive feedback loop to achieve phase inversion between the current and voltage, i.e. the voltage and current of the load resistance R_L are out of phase. As a result, assuming ideal transistors, the NIC resistance at the emitter nodes is given by:

$$R_{NIC} \approx \frac{2}{g_m} - R_L \tag{1}$$

Where g_m is the transconductance of the transistors. Clearly, if $R_L > 2/g_m$, then the overall resistance is negative. Accounting for the non-ideal intrinsic capacitances of the transistors will result in a frequency-dependent negative resistance in series with inductive reactance [12, 14, 21], such that the NIC impedance Z_{NIC} is given by:

$$Z_{NIC} = R_{NIC} + j\omega L_{NIC} \tag{2}$$

Hence, the NIC impedance Z_{NIC} can be emulated by a passive equivalent circuit that is a combination of negative resistance R_{NIC} in-series with inductance L_{NIC} as shown in Fig. 1. Such an inductive component will affect the integrity of the generated negative resistance and make it frequency-dependent. It will be possible to offset this undesirable effect

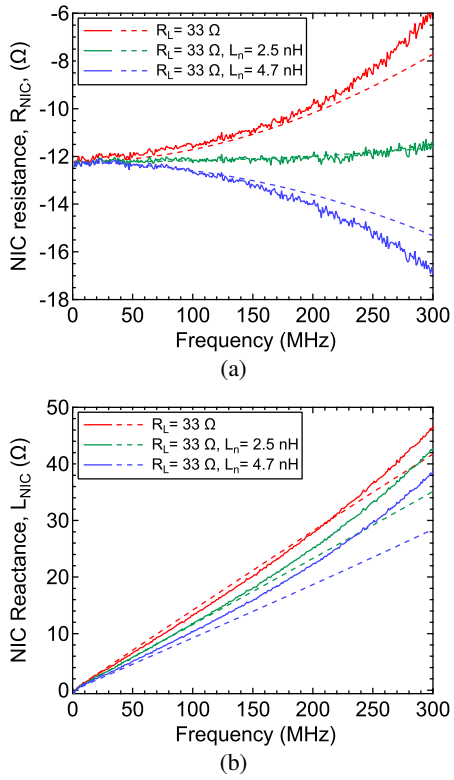

Fig. 2: Measured (solid) and simulated (dashed) NIC (a) resistance (b) reactance, with /without compensating inductance L_n

by placing a compensating inductor L_n in series with R_L so that the NIC generates negative inductance to cancel the effect of L_{NIC}.

It is worth noting that NICs are prone to instability due to the nature of their operation, which incorporates positive feedback. Therefore, to prevent NICs from oscillating, it is necessary to adhere to the stability criterion of the specific NIC configuration and carefully design the layout to minimise the length of the tracks, especially within the feedback loop, to avoid compromising the NIC stability. Extensive studies of NIC stability are covered in [13, 14].

Using discrete components, a negative resistance of $-12\ \Omega$ is generated. The NIC circuit in Fig. 1 was implemented on a FR4 printed circuit board (PCB) and populated using silicon NPN transistors BFR520U ($f_T = 10$ GHz) and surface mount devices (SMD) including all resistors and capacitors. The collector currents are set to $I_{C1} = I_{C2} = 3$ mA, at $V_{CC} = 6$ V. Whereas, $R_L = 33\ \Omega$, additional stabilising resistors, at the base of each transistor were used (not shown in Fig), $R_{stb} = 100\ \Omega$.

Despite being designed as a balanced configuration NIC, the initial measurements of the NIC circuit are conducted in the unbalanced (grounded) mode only (where one terminal of Z_{NIC} port is short circuited to ground). This is done to simplify the measurement process. To test the NIC performance, first, the return loss (S_{11}) of the fabricated NIC are measured using a vector network analyser (VNA). the S_{11} are

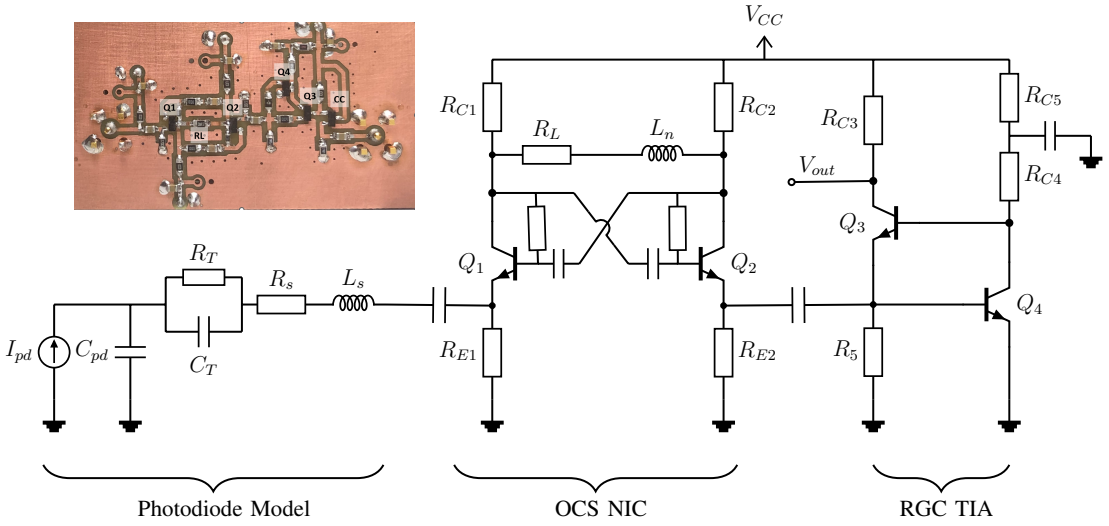

Fig. 3: Linvill OCS NIC circuit generating an in-series negative resistance to neutralise $R_s + R_T$, inset: Fabricated PCB

then converted into corresponding impedance parameters to obtain the real and imaginary parts of the NIC impedance.

The utility of the NIC circuit is demonstrated by plotting its negative resistance and inductive reactance. Moreover, the effect of offsetting the undesirable L_{NIC}, using the additional compensating inductor L_n is demonstrated for $L_n = 2.5$ nH and 4.7 nH. Fig. 2 shows the simulated and measured resistance and reactance of the NIC circuit with and without L_n. Clearly, measurements show good agreement with simulations. From Fig. 2a (red curve), it can be seen that the generated negative resistance starts at $-12\ \Omega$ and increases as a function of frequency. Such value is slightly different from the value given by (1), which is expected since (1) does not account for the non-ideal effect of the transistors and the additional resistors R_{stb}. Moreover, adding the compensating inductor $L_n = 2.5$ nH, reduces the frequency-dependent behaviour of the generated negative resistance to become nearly flat across the relevant frequency range. Such behaviour is reflected in Fig. 2b, the inductive reactance is reduced by adding L_n, which is a result of the compensation effect of L_n. Increasing L_n further skews the behaviour of the generated negative resistance, so it reduces as a function of frequency; such manipulation of R_{NIC} can aid in obtaining further bandwidth enhancement when connected between the photodiode and the TIA.

III. Application of NICs for Bandwidth Enhancement of VLC Receivers

This section investigates the effect of offsetting the photodiode series resistance on the bandwidth of VLC receivers. Initially, the photodiode equivalent circuit model is described. Subsequently, a design of a low input impedance TIA, namely the RGC TIA, is described. Finally, the bandwidth advantage of the NIC circuit is demonstrated in conjunction with the RGC TIA by implementing the circuit in Fig. 3.

A. Photodiode Passive Equivalent Circuit Model

This work adopts a photodiode passive equivalent model based on a verified model reported in [8]. From Fig. 3, it can be seen that the model accounts for the effect of C_{pd}, however, unlike the simplified models of [3–7, 11], it also considers the effect of R_s and the feed-line inductance L_s. In addition to, an RC combination R_T and C_T, which were attributed to contacts that are not fully ohmic and display some Schottky behaviour.

By analysing the stand-alone photodiode model in Fig. 3, when loaded by a TIA, it is clear that the sum of resistances $R_s + R_T$ is in series to the TIA input resistance R_a, such that the receiver's bandwidth can be approximated by:

$$BW \approx \frac{1}{2\pi(R_s + R_T + R_a)C_{pd}} \tag{3}$$

Clearly, $R_s + R_T$ impose an additional bandwidth-limiting factor on the receiver's bandwidth.

In this work, the bandwidth extension is achieved by neutralising the bandwidth-limiting effect of $R_s + R_T$ via a series negative resistance R_{NIC}. Ideally, if $R_{NIC} = R_s + R_T$, complete neutralisation of $R_s + R_T$ can be achieved, then the receiver's bandwidth would be solely dictated by the TIA input resistance R_a. Nevertheless, this would require the generation of pure negative resistance, with no associated reactance, whereas the NIC impedance is a combination of frequency dependent negative resistance in-series with the inductance L_{NIC}. Nevertheless, while complete neutralisation of $R_s + R_T$ is not practicable, yet optimisation is feasible to enhance the achievable bandwidth.

B. Low input impedance TIA design

In this work, a design example of an RGC TIA is briefly described, which is to be used as the TIA following the NIC. Fig. 3 shows the RGC configuration, which is widely described as a modification to the common base (CB) stage (Q_3) with feedback presented by a common emitter (CE) stage (Q_4); this has the benefit of reducing the input resistance by a factor approximately equals the voltage gain of the CE. Hence, the RGC input resistance R_a is given by:

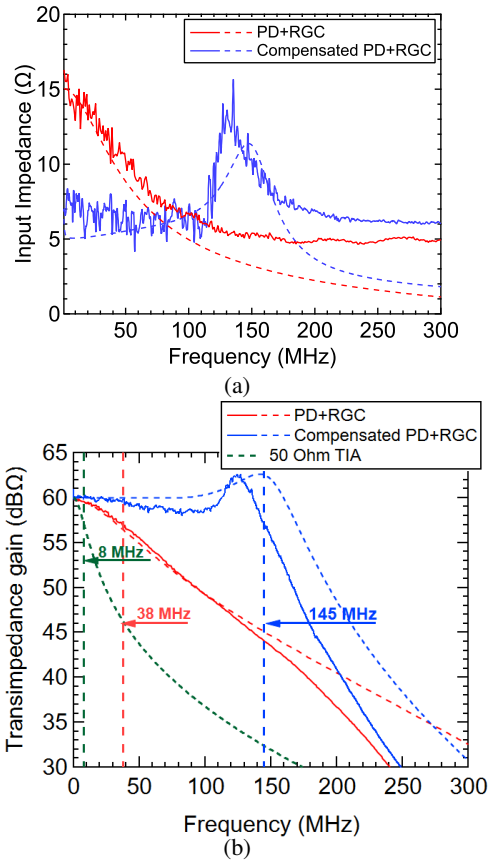

Fig. 4: Measured (solid) and simulated (dashed) responses of the RGC TIA and photodiode equivalent circuit with/without the negative resistance compensation (a) Input impedance (b) Transimpedance gain

$$R_a = \frac{1}{g_{m3}(1 + g_{m4}R_{C4})} \tag{4}$$

where g_{m3} and g_{m4} are the transconductances of Q_3 and Q_4, respectively, and R_{C4} is the load resistor of Q_4. Such configuration features ultra-low input resistance in the range of a few Ohms to a fraction of an Ohm, which offers high tolerance to exceptionally high C_{pd}. Details on the design of the RGC and a modified variant are studied in [6].

C. Negative resistance & Low input impedance TIA

This section illustrates the bandwidth advantage of neutralising the photodiode series resistances $R_s + R_T$. This is demonstrated by building two circuits on FR4 PCBs. First, the RGC TIA with the photodiode equivalent model and the second is the RGC TIA with the photodiode equivalent model and the intermediate negative resistance stage as shown by circuit in Fig. 3, each circuit is built with the addition of an output buffer-common collector (CC) stage.The PCBs are populated using the BFU520A transistors and SMD for resistors and capacitors. The values of the photodiode passive equivalent model were based on a verified model and parameter extraction of a commercially available silicon photodiode of area equals 100 mm^2, at a reverse bias voltage of 12 V reported in [8]. The parameter values are $C_{pd} = 300$ pF, $R_s = 9.1$ Ω, $R_T = 3.9$ Ω and $L_s = 10$ nH. The OCS NIC is biased at $I_{C1} = I_{C2} = 3$ mA and $R_L = 33$ Ω and $L_n = 15$ nH. The RGC is biased at $I_{C3} = 1$ mA, $I_{C4} = 4$ mA. The transimpedance gain is set by $R_{C3} = 1$ kΩ. Whereas, $R_{C4} = 150$ Ω at $V_{CC} = 6$ V.

Fig. 4 shows the measured and simulated responses of the RGC TIA with the photodiode equivalent circuit model with and without the negative resistance compensation. From Fig. 4a, it can be seen that the addition of the OCS NIC stage results in a significant reduction of the input resistance in relative to the RGC input impedance with the photodiode equivalent circuit only. For the RGC and the photodiode equivalent model, the resistance is approximately 15 Ω, corresponding to $R_s + R_T + R_a$. The addition of the OCS NIC reduces the input resistance so that it is approximately 7 Ω, which corresponds to $R_s + R_T + R_{NIC} + R_a$. Hence, the OCS NIC results in effective neutralisation of $R_s + R_T$. Nevertheless, such reduction in the input resistance is also accompanied by frequency peaking. This peaking is a result of the complex nature of the RGC input dominant pole [6], this is, in addition to, the interplay of the NIC inductance L_{NIC} with the RGC TIA, which also leads to the peaking effect. Therefore, care must be taken to choose optimum value of R_L and L_n to avoid excessive peaking.

The bandwidth advantage of offsetting $R_s + R_T$ is reflected in the transimpedance gain frequency responses shown by Fig. 4b. Our compensation technique achieves substantial bandwidth enhancement of nearly 400%, relative to the uncompensated RGC TIA. Such enhancement is due to the reduction in the photodiode series resistance at the TIA input, which pushes its dominant input complex pole to higher frequencies. It is worth noting that the differences observed between the simulated and measured frequency responses are due to additional parasitic effects from the fabricated PCB, which can be eliminated with improved PCB layout design and fabrication. The bandwidth advantage of our compensation technique is further accentuated by simulating the frequency response of a 50 Ω input impedance TIA using the same photodiode model in [8] (shown by green curve in Fig. 4b), resulting in only 8 MHz as determined by (3), as such our proposed circuit offers substantial bandwidth improvement for VLC receivers of more than 1800% compared to traditional 50 Ω input impedance TIAs.

IV. Conclusion

This work reports the design and verification of a NIC circuit to generate floating negative resistance to neutralise the bandwidth limiting effect of the photodiode series resistance, thereby extending the bandwidth of optical receivers. The NIC performance is evaluated through the measurement of the scattering parameters of a circuit constructed using discrete components on a PCB. We demonstrate the bandwidth advantage of the NIC by applying it to a photodiode equivalent model, in conjunction with a low input impedance TIA, which yields substantial bandwidth enhancement.

REFERENCES

[1] Z. Ghassemlooy, L. N. Alves, S. Zvanovec, and M.-A. Khalighi, *Visible light communications: theory and applications*. CRC press, 2017.

[2] R. Aguiar, A. Tavares, J. Cura, E. De Vaaconcelos, L. Alves, R. Valadas, and D. Santos, "Considerations on the design of transceivers for wireless optical LANs," in *IEE Colloquium on Optical Wireless Communications*, 1999, pp. 2/1–231.

[3] J. L. Cura and L. N. Alves, "Bandwidth improvements in transimpedance amplifiers for visible-light receiver front-ends," in *2013 IEEE 20th International Conference on Electronics, Circuits, and Systems (ICECS)*, 2013, pp. 831–834.

[4] B. Huang and H. Chen, "A monolithic optical receiver chip for free space visible light communication system," in *2012 IEEE 11th International Conference on Solid-State and Integrated Circuit Technology*, 2012, pp. 1–3.

[5] R. Y. Chen and Z.-Y. Yang, "CMOS transimpedance amplifier for visible light communications," *IEEE Transactions on Very Large Scale Integration (VLSI) Systems*, vol. 23, no. 11, pp. 2738–2742, 2015.

[6] A. Kassem and I. Darwazeh, "Practical demonstration of RGC and modified RGC TIAs for VLC systems," in *2021 28th IEEE International Conference on Electronics, Circuits, and Systems (ICECS)*, 2021, pp. 1–6.

[7] E. S. Parapari, E. S. Parapari, and Z. D. Koozehkanani, "A broadband transimpedance amplifier (TIA) for visible light communication in $0.18\ \mu\mathrm{m}$ CMOS," in *2020 28th Iranian Conference on Electrical Engineering (ICEE)*, 2020, pp. 1–4.

[8] A. Kassem and I. Darwazeh, "Equivalent circuit model for large-area photodiodes for VLC systems," in *2022 13th International Symposium on Communication Systems, Networks and Digital Signal Processing (CSNDSP)*, 2022, pp. 467–472.

[9] Z. Xu and J. Gao, "Semi-analytical small signal parameter extraction method for pin photodiode," *IET Optoelectronics*, vol. 11, no. 3, pp. 103–107, 2017.

[10] A. Steinbach, I. Penn, N. Chokshi, D. Martin, K. Slomkowski, W. Baun, N. Agrawal, R. Ben-Michael, and M. Itzler, "Equivalent circuit modelling of p-i-n photodiodes for 40 Gb/s receivers," in *The 15th Annual Meeting of the IEEE Lasers and Electro-Optics Society*, vol. 2, 2002, pp. 486–487 vol.2.

[11] E. Säckinger, "The transimpedance limit," *IEEE Transactions on Circuits and Systems I: Regular Papers*, vol. 57, no. 8, pp. 1848–1856, 2010.

[12] J. Linvill, "Transistor negative-impedance converters," *Proceedings of the IRE*, vol. 41, no. 6, pp. 725–729, 1953.

[13] Q. Tang and H. Xin, "Stability analysis of non-foster circuit using normalized determinant function," *IEEE Transactions on Microwave Theory and Techniques*, vol. 65, no. 9, pp. 3269–3277, 2017.

[14] B. Buiantuev, N. Kalmykov, D. Kholodnyak, A. Brizić, L. Vincelj, and S. Hrabar, "Physically oriented design of negative capacitors based on linvill's floating impedance converter," *IEEE Transactions on Microwave Theory and Techniques*, vol. 70, no. 1, pp. 139–154, 2022.

[15] A. Larky, "Negative-impedance converters," *IRE Transactions on Circuit Theory*, vol. 4, no. 3, pp. 124–131, 1957.

[16] A. Kassem and I. Darwazeh, "Use of negative impedance converters for bandwidth extension of optical transmitters," *IEEE Open Journal of Circuits and Systems*, vol. 2, pp. 101–112, 2021.

[17] A. N. Beal, J. N. Blakely, and N. J. Corron, "Extended-bandwidth negative impedance converters by nested networks," *IEEE Transactions on Circuits and Systems II: Express Briefs*, vol. 65, no. 9, pp. 1134–1138, 2018.

[18] J. Han, K. Yoo, D. Lee, K. Park, W. Oh, and S. M. Park, "A low-power gigabit CMOS limiting amplifier using negative impedance compensation and its application," *IEEE Transactions on Very Large Scale Integration (VLSI) Systems*, vol. 20, no. 3, pp. 393–399, 2012.

[19] A. Ghadiri and K. Moez, "Gain-enhanced distributed amplifier using negative capacitance," *IEEE Transactions on Circuits and Systems I: Regular Papers*, vol. 57, no. 11, pp. 2834–2843, 2010.

[20] S. E. Sussman-Fort and R. M. Rudish, "Non-foster impedance matching of electrically-small antennas," *IEEE Transactions on Antennas and Propagation*, vol. 57, no. 8, pp. 2230–2241, 2009.

[21] C. R. White, J. S. Colburn, and R. G. Nagele, "A non-foster vhf monopole antenna," *IEEE Antennas and Wireless Propagation Letters*, vol. 11, pp. 584–587, 2012.